

# Single-Molecule Imaging of RNA Polymerase-DNA Interactions in Real Time

Yoshie Harada,\* Takashi Funatsu,\* Katsuhiko Murakami,# Yoshikazu Nonoyama,\$ Akira Ishihama,# and Toshio Yanagida\*<sup>§</sup> <sup>†</sup>

\*BioMotron Project, ERATO, JST, Senba-Higashi 2-4-14, Mino, Osaka 562-0035; #Department of Molecular Genetics, National Institute of Genetics, Mishima, Shizuoka 411-0801; \$Department of Biophysical Engineering, Faculty of Engineering Science, Osaka University, Toyonaka, Osaka 560-0043; and <sup>†</sup>Department of Physiology, Medical School, Osaka University, Suita, Osaka 565-0871, Japan

**ABSTRACT** Using total internal reflection fluorescence microscopy, we have directly observed individual interactions of single RNA polymerase molecules with a single molecule of  $\lambda$ -phage DNA suspended in solution by optical traps. The interactions of RNA polymerase molecules were not homogeneous along DNA. They dissociated slowly from the positions of the promoters and sequences common to promoters at a rate of  $\sim 0.66 \text{ s}^{-1}$ , which was more than severalfold smaller than the rate at other positions. The association rate constant for the slow dissociation sites was  $9.2 \times 10^2 \text{ bp}^{-1} \text{ M}^{-1} \text{ s}^{-1}$ . The frequency of binding to the fast dissociation sites was dependent on the A-T composition; it was larger in the AT-rich regions than in the GC-rich regions. RNA polymerase molecules on the fast dissociation sites underwent linear diffusion (sliding) along DNA. The binding to the slow dissociation sites was greatly enhanced when DNA was released to a relaxed state, suggesting that the binding depended on the strain exerted on the DNA. The present method is potentially applicable to the examination of a wide variety of protein–nucleic acid interactions, especially those involved in the process of transcription.

## INTRODUCTION

The first step of gene expression is the binding of RNA polymerase molecules to DNA and its search for the gene promoter. This step is the center of the regulatory mechanism of transcription and has been extensively investigated, mainly by kinetic (McClure, 1985; Singer and Wu, 1987; Ricchetti et al., 1988; Spolar and Record, Jr., 1994) and structural (Polyakov et al., 1995; Werner et al., 1996) studies. The kinetic studies have proposed some mechanisms for promoter searching based on the results of the binding of RNA polymerase molecules to specific and nonspecific sites on the DNA: sliding (one-dimensional diffusion of nonspecific binding proteins along the DNA), intersegment transfer (direct intersegment transfer of proteins between nonspecific DNA sites within the domain), and simple dissociation-association reactions (three-dimensional diffusion in solution) (von Hippel and Berg, 1989). Fluid tapping-mode atomic force microscopy has allowed the initiation (formation of the open complex) and elongation in the transcription process to be directly observed in sequential images (Rees et al., 1993; Kasas et al., 1997; Rippe et al., 1997).

Recently, new optical methods for imaging (Matsumoto et al., 1981) and manipulating (Perkins et al., 1994) DNA have opened a new phase in the study of gene expression. Detailed elastic characteristics of DNA have been examined by manipulating a single molecule of DNA with an optical trap and a microneedle (Cluzel et al., 1996; Smith et al.,

1996; Wang et al., 1997). Single-molecule processes of transcription by RNA polymerase have been detected by monitoring a tag attached to DNA (Schafer et al., 1991; Yin et al., 1995). Kabata and co-workers have observed movement of single RNA polymerase molecules, conjugated with avidin labeled with many fluorescent dye molecules, in a bundle of extended DNA molecules under a conventional optical microscope (Kabata et al., 1993). Their results support sliding as a mechanism for searching the promoter. We have demonstrated that single fluorophores can be clearly observed in aqueous solution by total internal reflection fluorescence microscopy, refined so that the background light is very low (Funatsu et al., 1995; Vale et al., 1996; Harada et al., 1998). By combining this technique with the manipulation of DNA by optical traps, we have developed a new system in which individual interactions of single RNA polymerase molecules with a single molecule of DNA suspended in solution can be directly observed in real time.

## MATERIALS AND METHODS

### Preparation of DNA conjugated with beads

Streptavidin-coated beads were prepared according to the method of Berliner and colleagues (Berliner et al., 1995), with some modifications. Biotin-x-cadaverine (0.78 mg/ml; Molecular Probes, Eugene, OR) was conjugated to 1  $\mu\text{m}$  carboxylated polystyrene beads (2% w/v; Bangs Laboratories, Carmel, IN) in a solution containing 5 mg/ml of 1-ethyl-3-(3-dimethylaminopropyl)carbodiimide HCl, 6 mg/ml of *N*-hydroxysulphosuccinimide, and 20 mM sodium phosphate, pH 7.0. After 1 h, the reaction was quenched by the addition of 10 mM glycine, pH 8.0. Free cross-linker was removed from the solution by successive centrifugation and pelleting of the microspheres. Biotinylated beads were suspended in 2 mg/ml of streptavidin, 10 mM HEPES, pH 7.8, 100 mM KCl, and 1 mM EDTA and stored on ice. Before use, unbound streptavidin was removed from the beads by washing. Biotinylated oligonucleotides complementary to both cohesive ends of the  $\lambda$ -phage DNA (Takara Biochemicals, Japan) were

Received for publication 7 July 1998 and in final form 8 October 1998.

Address reprint requests to Dr. Yoshie Harada, Department of Physics, Keio University, 3-14-1 Hiyoshi, Kohoku-ku, Yokohama 223-8522, Japan. Tel.: 81-44-750-1710; Fax: 81-44-750-1712; E-mail: harada@phys.keio.ac.jp.

© 1999 by the Biophysical Society

0006-3495/99/02/709/07 \$2.00

ligated on to the  $\lambda$ -phage DNA (Takara Biochemicals). Streptavidin-coated beads (in 0.5  $\mu$ l of 10 mM HEPES, pH 7.8, 100 mM KCl, 1 mM EDTA) were incubated with biotinylated  $\lambda$ -phage DNA (470 pM in 0.5  $\mu$ l of 10 mM HEPES, pH 7.8, 100 mM KCl, 1 mM EDTA). A flow cell (Iwane et al., 1997) was rinsed with 2 mg/ml of  $\alpha$ -casein in 10 mM HEPES, pH 7.8, 100 mM KCl, 1 mM EDTA; incubated for several minutes; and rinsed twice with a solution containing 20 mM HEPES, pH 7.8, 100 mM KCl, 1 mM  $\text{MgCl}_2$ , 50% sucrose, 0.5% 2-mercaptoethanol, and an oxygen scavenger system (Harada et al., 1990). Rinse volumes were 10  $\mu$ l. Beads conjugated with DNA were then diluted in 10  $\mu$ l of 9 nM fluorescently labeled RNA polymerase molecules in 20 mM HEPES, pH 7.8, 100 mM KCl, 1 mM  $\text{MgCl}_2$ , 50% sucrose, 0.5% 2-mercaptoethanol, and an oxygen scavenger system. Pretreatment of the glass surface with  $\alpha$ -casein and 50% sucrose was essential for low nonspecific binding of RNA polymerase molecules to the glass surface. An unlabeled DNA molecule that had beads bound at both ends was selected and suspended near the surface of a pedestal by manipulating the beads with dual optical traps under bright-field illumination. The concentration of DNA was low (see above), so that only a few beads out of >1000 beads were connected with other beads through the DNA. Therefore, there should be a negligibly small possibility that more than one DNA molecule was suspended between two beads. This point was confirmed by directly observing the DNA after fluorescent labeling with TOTO-1 (Molecular Probes).

### Preparation of fluorescently labeled RNA polymerase molecules

*Escherichia coli* core RNA polymerase is composed of two  $\alpha$ -subunits, one  $\beta$ -subunit, and one  $\beta'$ -subunit. The cysteine residues of the  $\alpha$ -subunit of an RNA polymerase molecule, except for 269C, were replaced with alanine. Mutant  $\alpha$ ([269C] $\alpha$ -),  $\beta$ -,  $\beta'$ -, and  $\sigma^{70}$ -subunits were expressed and purified according to the methods of Igarashi and Ishihama (1991). The 269C residue of the [269C]  $\alpha$ -subunit was labeled with Cy3-maleimide. Cy3-maleimide was synthesized from Cy3-OSu (Amersham Pharmacia Biotech, Arlington Heights, IL) by incubation with *N*-(2-(1-piperazinyl)ethyl)maleimide (Dojindo Laboratories, Japan) for 8 h at 40°C. The [269C]  $\alpha$ -subunit was mixed with Cy3-maleimide in a ratio of 1:10 in 10 mM Tris-Cl, pH 8.0, 5% glycerol, 0.1 mM EDTA for 1 h at 37°C. Unbound dyes were removed by gel filtration. The molar ratio of  $\alpha$ -subunit: Cy3 was 1:0.5. Reconstitution and separation of assembled enzymes from unassembled subunits was carried out as previously described (Igarashi and Ishihama, 1991). RNA polymerase core enzyme activity was assayed under standard conditions (Igarashi and Ishihama, 1991). The core enzyme activity after fluorescent labeling was 96% of that before labeling. Holoenzymes were prepared by mixing the reconstituted core enzymes with a sixfold molar excess of purified  $\sigma^{70}$  and incubating for 15 min at 30°C in 10 mM Tris-Cl, pH 7.6, 10 mM  $\text{MgCl}_2$ , 20 mM NaCl, 0.1 mM EDTA, 1 mM dithiothreitol, and 50% glycerol. All experiments were performed at 25°C.

### Optics

A total internal reflection microscope used to visualize single fluorophores (Funatsu et al., 1995) was modified to accommodate dual optical traps. The optical trap used a diode-pumped Nd:YAG infrared laser (wavelength 1064 nm, 7910-Y4-106; Spectra-Physics Lasers, Mountain View, CA). Two traps were produced by passing the laser beam through a quarter-wave plate followed by a polarizing beam splitter. One of the beams was deflected with two orthogonal scanners that were operated with the mouse of a computer. Microbeads were illuminated with infrared light (700–800 nm) from a halogen lamp. A beam splitter was used to produce two images of the beads. One image was captured by a CCD camera. The other was projected onto a quadrant photodiode detector to monitor the stiffness by measuring displacements of one of the beads in two dimensions as described previously (Higuchi et al., 1997). The trapping stiffness (0.06 pN/nm) was determined from thermal fluctuations of trapped beads by using the equipartition law (Svoboda et al., 1993). The force applied to

DNA ( $\sim 5$  pN) was determined by measuring the displacements of the bead from the center of the trap with nanometer accuracy (Finer et al., 1994). As the bead undergoes free thermal rotation in the trap at an applied force of several pN (Tsuda et al., 1996), rotational strain exerted on the DNA by pulling it taut would be negligibly small. Fluorophores were excited with a frequency-doubled Nd:YAG laser (wavelength 532 nm, model 140-0534-200; Light Wave Electronics, Mountain View, CA). Fluorescence images were captured by a silicon-intensified target camera (C2741; Hamamatsu Photonics, Hamamatsu, Japan) coupled to an image intensifier (VS4-1845; Video Scope International, Sterling, VA) and recorded on videotape. Bright-field images of the beads and fluorescence images of Cy3-labeled RNA polymerase molecules could be observed simultaneously. An oil-immersion objective lens (Plan NCF Fluor  $\times 100$ , 1.3 NA; Nikon, Tokyo) was used.

## RESULTS AND DISCUSSION

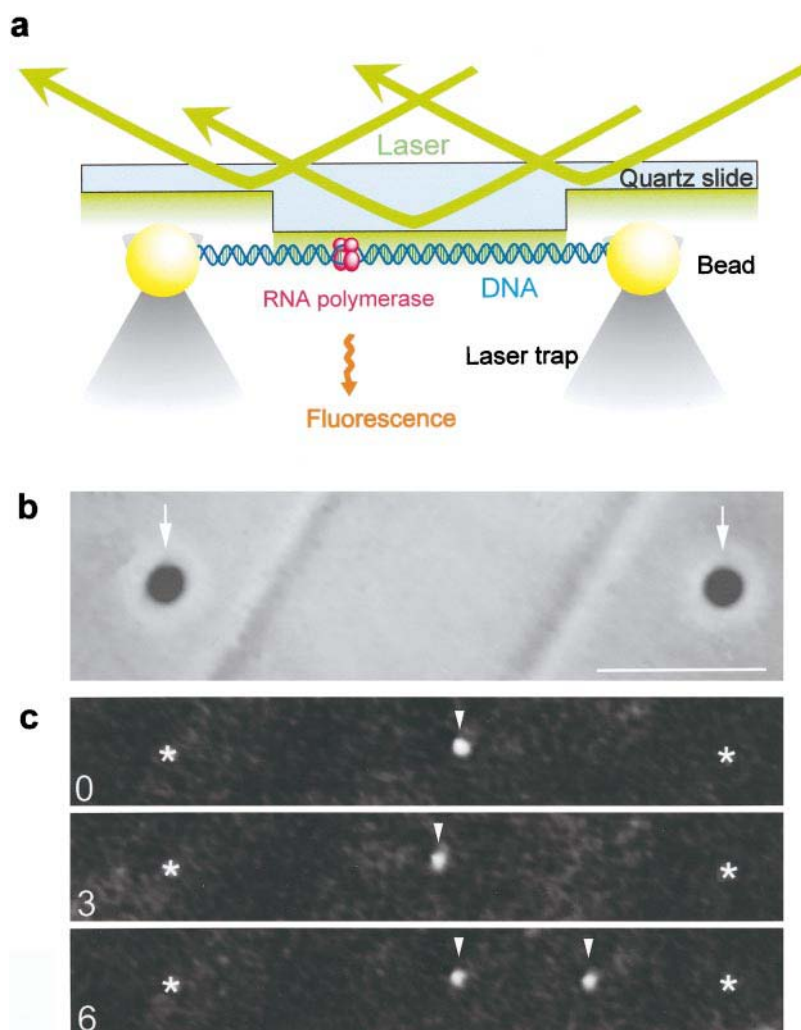
### Observations

Fig. 1 *a* shows a schematic drawing of the experimental arrangement. An unstained  $\lambda$ -phage DNA molecule with both ends attached to beads was captured and stretched to full extension by dual optical traps under bright-field illumination. The tension exerted on the DNA was  $\sim 5$  pN in all experiments, except for those in Fig. 6. The DNA was brought near the surface of a rectangular pedestal 8  $\mu$ m wide and 2  $\mu$ m deep, which had been made on a glass surface by chemical etching (Ishijima et al., 1998). Individual interactions of single fluorescently labeled RNA polymerase molecules with the DNA were directly observed by the evanescent field produced when a laser was totally reflected in the interface between the glass and the solution (Funatsu et al., 1995). Fig. 1 *b* shows the bright-field image of the beads in the optical traps, between which a single DNA molecule has been suspended. An oblique band between the beads indicates a part of the rectangular pedestal. Fig. 1 *c* shows the fluorescence image of the same field as in Fig. 1 *b* when the bright-field illumination was switched to the evanescent field illumination. Arrowheads show single RNA polymerase molecules bound to the DNA at the times indicated. The fluorescence of a surface-adsorbed RNA polymerase molecule disappeared primarily in either a one-step or a two-step process, as expected for photobleaching reactions of one or two dye molecules, respectively, bound to the two  $\alpha$ -subunits of RNA polymerase. The distribution of fluorescence intensities of the spots was similar at various concentrations of KCl in the range of 10–100 mM. Brighter spots due to large aggregations of molecules were very few in number (<5% of observed spots) and could easily be identified by eye. The position of the RNA polymerase molecules bound to a suspended DNA was determined frame by frame, and the centroid of the fluorescent spots was calculated with an image processor. The resolution was  $\sim 0.2$   $\mu$ m.

### Localization

The histogram in Fig. 2 *a* shows the localization of RNA polymerase molecules bound to the  $\lambda$ -phage DNA. The

**FIGURE 1** Imaging of individual interactions of single molecules of RNA polymerase with a single DNA molecule. (a) Schematic drawing of experimental arrangement (not drawn to scale). See text for explanation. (b) Bright-field images of the beads in optical traps. A single  $\lambda$ -phage DNA molecule is suspended between the beads (marked by *arrows*), although it cannot be observed directly. An oblique band between the beads indicates the rectangular pedestal on the glass surface. (c) Fluorescence images of the field in *b*. Arrowheads indicate single molecules of fluorescently labeled RNA polymerase bound to the DNA (time in seconds). Asterisks (\*) show the positions of the beads. The DNA cannot be observed because it is not fluorescently labeled. The rate of photobleaching was  $0.03 \text{ s}^{-1}$ , or the lifetime of the fluorophore was, on average, 30 s. The concentration of RNA polymerase was low (9 nM), so that usually no more than two polymerase molecules bound to the DNA at any given time. Bar,  $5 \mu\text{m}$ .



extended length of the  $\lambda$ -phage DNA used was  $\sim 16 \mu\text{m}$ . The base composition of DNA is shown in Fig. 2 *b*. RNA polymerase molecules bound more frequently to AT-rich regions than to GC-rich regions. In some cases, RNA polymerase molecules bound about fourfold more frequently to the DNA at 11–12.5  $\mu\text{m}$  from the left bead than at the corresponding symmetric position, 3.5–5  $\mu\text{m}$ . In other cases, the reverse was found to be true. Thus it was easy to identify the orientation of the DNA suspended between the beads. As the RNA polymerase should have higher affinity for its promoters (11.7 and 12.5  $\mu\text{m}$ ), the orientation of the DNA was determined so that the region where RNA polymerase molecules most frequently bound to the DNA coincided with its promoter positions (Figs. 2 and 4). A histogram of the lifetimes of RNA polymerase molecules bound to the AT-rich regions of DNA fits a function of two exponentials,  $N = 281 \exp(-3.0t) + 19 \exp(-0.66t)$  (Fig. 3). The rates were  $3.0 \text{ s}^{-1}$  for the fast dissociation and  $0.66 \text{ s}^{-1}$  for the slow dissociation. A major component of the histogram of the lifetimes of RNA polymerase molecules bound to the GC-rich regions (not shown) could be fitted by a single exponential with a dissociation rate constant of  $8.4 \text{ s}^{-1}$ , which corresponds to that for the fast dissociation in the

AT-rich regions. The rate for slow dissociation could not be determined because the frequency was too small. The association rate constants in the fast and slow dissociation sites were also determined. As the rate of sudden disappearance of the spots of RNA polymerase molecules on the glass surface (photobleaching), determined as previously described (Tokunaga et al., 1997), was  $0.03 \text{ s}^{-1}$  (or the mean lifetime of fluorophores was 30 s), the effect of photobleaching was negligible; the probability that photobleaching occurred before dissociation was calculated as  $\sim 1 - \exp(-0.03 \text{ s}^{-1}/(0.66-8.4) \text{ s}^{-1}) \leq \sim 5\%$  (Ishijima et al., 1998). The results are summarized in Table 1. For the fast dissociation sites, the association was one order of magnitude slower and the dissociation was one order of magnitude faster, respectively, than those estimated by kinetic studies (Singer and Wu, 1987). This difference may be due to the fact that the DNA was stretched in this study. More RNA polymerase molecules were found to bind to the DNA when it was relaxed, as shown later (see Fig. 6), supporting this idea.

Fig. 4 *a* indicates the localization of RNA polymerase molecules that remained bound to the DNA for more than 1.5 s. Most of RNA polymerase molecules that remained bound for  $>1.5 \text{ s}$  should bind to the slow dissociation sites



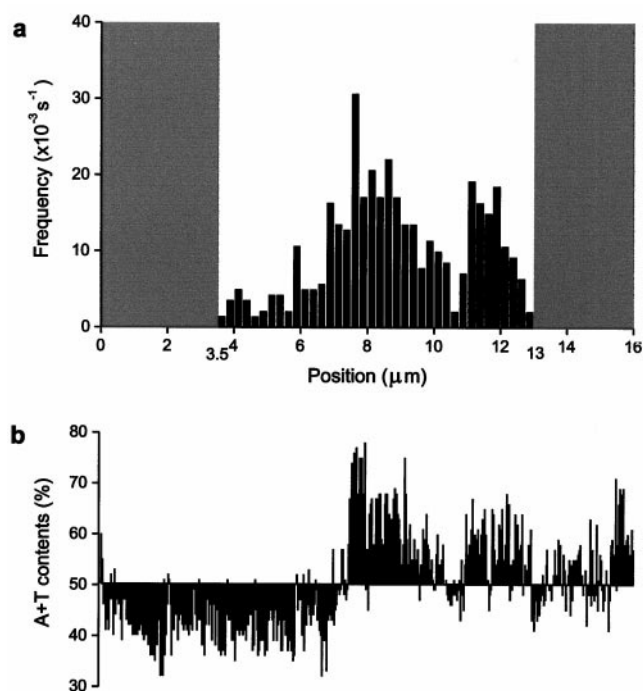


FIGURE 2 Localization of RNA polymerase molecules bound to  $\lambda$ -phage DNA. (a) Histogram of the frequency of binding of RNA polymerase molecules to  $\lambda$ -phage DNA. The number of RNA polymerase molecules interacting with DNA for a unit period was counted every 0.25  $\mu\text{m}$ . The left and right ends of  $\lambda$ -phage DNA are denoted as 0 and 16  $\mu\text{m}$ , respectively. The regions from 0 to 3.5  $\mu\text{m}$  and from 13 to 16  $\mu\text{m}$  (gray regions) were out of the evanescent field, so the binding of RNA polymerase molecules was not observed. RNA polymerase molecules underwent linear diffusion along DNA (see Fig. 5). The fraction of RNA polymerase molecules that slid along the DNA over  $>0.2 \mu\text{m}$  was  $\sim 2.5\%$ , so we did not consider the effect of the sliding on the binding position. The total number of RNA polymerase molecules observed was 570. (b) Percentage of A + T contents of  $\lambda$ -phage DNA in windows of 100 bases. The average is 50.1%.

as defined above, because more than 99% of RNA polymerase molecules bound to the fast dissociation sites should dissociate from DNA within 1.5 s (Fig. 3). Many RNA polymerase molecules remained bound to the region of the DNA between 11.5 and 13  $\mu\text{m}$ . The  $\lambda$ -phage DNA has two promoters,  $P_L$  and  $P_R$ , located near the 35,600 base and the 38,000 base, which correspond to lengths of 11.7 and 12.5  $\mu\text{m}$ , respectively. The positions of the promoters correspond to the region where the RNA polymerase molecules remained bound for a long time. Thus the slow dissociation should be due to the specific binding of RNA polymerase molecules to the promoters. High-affinity regions also exist near the center of the  $\lambda$ -phage DNA. Promoter-like sequences exist in this region (Fig. 4 b), even though no promoter could be identified. It is possible that RNA polymerase molecules remained bound to these pseudopromoters for long periods of time. The role of the pseudopromoters is not known.

### Linear diffusion

Some of the RNA polymerase molecules on the fast dissociation sites moved along the DNA (Fig. 5). The direction of

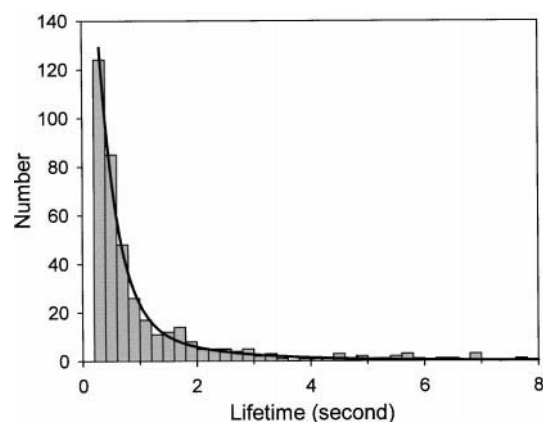


FIGURE 3 Histogram of the lifetimes of RNA polymerase molecules bound to the AT-rich regions of  $\lambda$ -phage DNA. A solid line shows a best fit to two exponentials,  $281 \exp(-3.0t) + 19 \exp(-0.66t)$ . See text for detail.

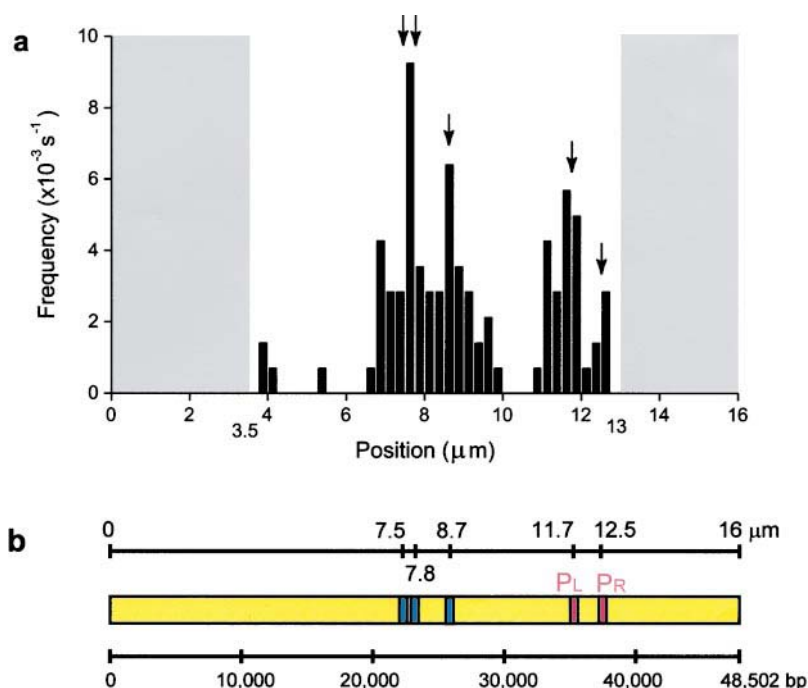
movement along the DNA was random, indicating that the movement was due to thermal diffusion. This observation provides direct evidence of the linear diffusion of single molecules of RNA polymerase, bound to the fast dissociation sites, along a single DNA molecule. The fraction of RNA polymerase molecules that diffused further than the present space resolution ( $\sim 0.2 \mu\text{m}$ ; see above) was 10 out of 381 molecules analyzed by the image processor. Assuming that other RNA polymerase molecules underwent thermal diffusion, but their diffusion could not be observed

TABLE 1 Association and dissociation rate constants of RNA polymerase at fast and slow dissociation sites of  $\lambda$ -phage DNA

	$k_{\text{off}} (\text{s}^{-1})$	$k_{\text{on}} (\text{bp}^{-1} \text{M}^{-1} \text{s}^{-1})$
AT fast	3.0	$2.4 \times 10^3$
AT slow	0.66	$9.2 \times 10^2$
GC fast	8.4	$1.8 \times 10^3$
GC slow	ND	ND

The histogram of the lifetimes of RNA polymerase molecules bound to the AT-rich regions of DNA fits the sum of two exponentials,  $281 \exp(-3.0t) + 19 \exp(-0.66t)$  (Fig. 3). The dissociation rate constants were obtained from the time constants of the two components. The fast and slow components correspond to dissociation at fast and slow dissociation sites, respectively (see text for details). The association rate constants were obtained as  $(\text{number of RNA polymerase molecules bound to DNA}) \times (\text{number of base pairs})^{-1} \times (\text{observation time})^{-1} \times (\text{concentration of RNA polymerase})^{-1}$ . The number of RNA polymerase molecules that bound to fast and slow dissociation sites of DNA for the observation time (1400 s) were 529 and 200, respectively, as determined from the histograms. Other numerical values: number of base pairs at AT-rich region = 17,400; concentration of RNA polymerase = 9 nM. A histogram of the lifetimes of RNA polymerase molecules bound to GC-rich regions of DNA (not shown) was fitted to a single exponential of  $110 \exp(-8.4t)$ . Only the rate constants at the fast dissociation sites were determined, because the frequency of the association at the slow dissociation sites was too small to be analyzed. Rate constants were determined in the same manner as the AT-rich regions. Numerical values specific to GC-rich regions: number of RNA polymerase molecules that bound to fast dissociation sites = 149; number of base pairs at GC-rich region = 6700. ND, Not determined.

FIGURE 4 Localization of RNA polymerase molecules bound to  $\lambda$ -phage DNA for more than 1.5 s (a) Histogram of the number of RNA polymerase molecules bound to DNA. Arrows indicate the positions of the promoters and pseudopromoters, as shown in b. Bin width, 0.25  $\mu\text{m}$ . (b) Positions of the promoters ( $P_L$ ,  $P_R$ ) and sequences common to promoters (pseudopromoters, blue-black strips). Sequences common to promoters were searched according to the method of McClure (1985).



because of the small diffusion range ( $<0.2 \mu\text{m}$ ), and the polymerase molecules have the same average behavior independent of the local sequence of the DNA, then the diffusion constant  $D$  can be estimated to be on the order of  $10^{-10} \text{ cm}^2 \text{ s}^{-1}$  by inserting the average lifetime of fast dissociation sites  $t_o = 0.2 \text{ s}$  ( $1/3.0 \text{ s}^{-1}$ ) into the equation (Berg, 1983)  $2 \int_{0.2 \mu\text{m}}^{\infty} (1/\sqrt{4\pi Dt_o}) \exp(-x^2/4Dt_o) dx = 10/381$ . This diffusion constant is one to three orders of magnitude smaller than those predicted by kinetic studies (Singer and Wu, 1987; McClure, 1985). This difference may be due to the fact that we stretched the DNA in this study or the prediction used to determine the diffusion coefficient in the kinetic studies might be incorrect. The average range of linear diffusion for the lifetime of binding

( $\sim 0.2 \text{ s}$ ) has been calculated as  $\langle x^2 \rangle^{1/2} = (2Dt_o)^{1/2} \approx 90 \text{ nm}$ , i.e., 300 bp. The probability of RNA polymerase molecules binding to the promoters would be increased by diffusion along DNA, compared to polymerase undergoing random association/dissociation (hopping) along the DNA (Singer and Wu, 1987; Ricchetti et al., 1988; von Hippel and Berg, 1989; Kabata et al., 1993).

### Enhanced binding to relaxed DNA

DNA forms a random coil structure in its physiological state. Therefore, we examined the binding of RNA polymerase molecules to DNA when it was released to a relaxed state. Fig. 6 shows the change in the number of RNA polymerase molecules bound to the DNA after the relaxed DNA had been extended. Many RNA polymerase molecules remained bound to the DNA for 1–2 s after extension (Fig. 6, upper panel). Bound RNA polymerase molecules gradually dissociated from the extended DNA, and new polymerase molecules bound to it at a steady rate (Fig. 6, middle and lower panels). The positions of the majority of the bound RNA polymerase molecules after extension of the DNA coincided with the slow dissociation sites observed in Fig. 4 a. The lifetime of the binding was as long as that for the slow dissociation sites, indicating that the bound polymerase molecules observed should be trapped in the slow dissociation sites of the DNA. Thus the specific binding of RNA polymerase molecules to the promoters and sequences common to promoters was enhanced when DNA was in a relaxed state. This may be because the relaxed DNA could wrap around the RNA polymerase, and thus the RNA polymerase bound more steadily to the DNA (Rippe et al., 1997; Craig et al., 1995; Giladi et al., 1996; Tang et al., 1996).

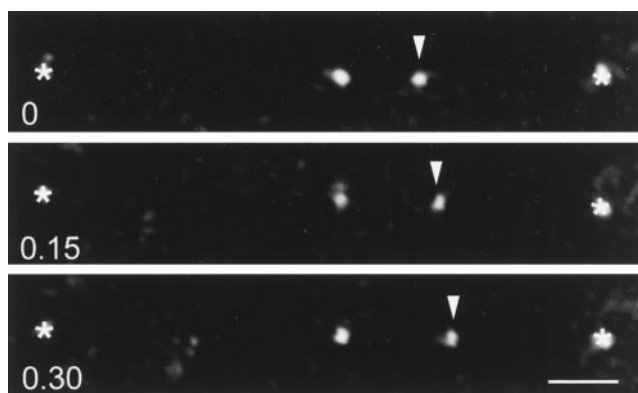


FIGURE 5 Linear diffusion of an RNA polymerase molecule along DNA. Arrowheads track a diffusing fluorescently labeled RNA polymerase molecule along DNA (time in seconds), and asterisks (\*) mark the beads in the optical traps. A stationary fluorescent spot shows an RNA polymerase molecule trapped in a pseudopromoter. Bar, 2  $\mu\text{m}$ .

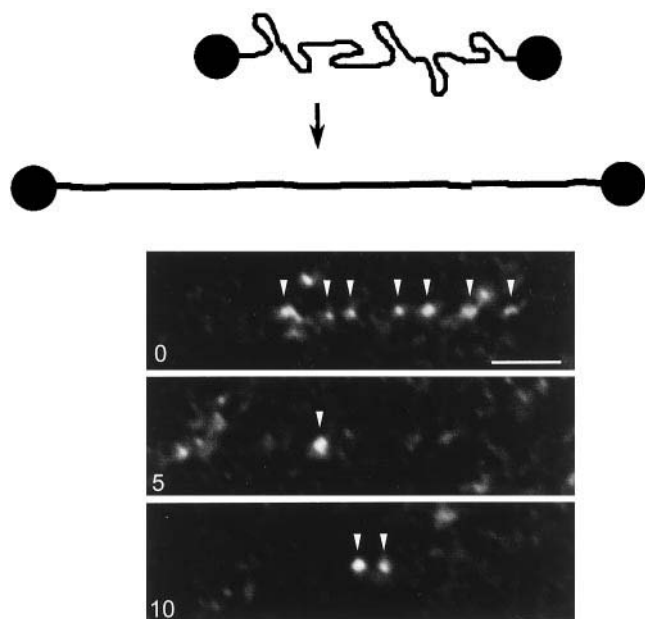


FIGURE 6 Enhanced binding of RNA polymerase molecules to relaxed DNA. The DNA was relaxed to 8  $\mu\text{m}$  in length and allowed to interact with RNA polymerase molecules in solution for several minutes. The upper panel shows a fluorescence image of RNA polymerase molecules (marked by arrowheads) bound to the DNA just after the DNA was extended to full length. The middle and lower panels show the fluorescence images of RNA polymerase molecules (marked by arrowheads) newly bound to the extended DNA after 5 and 10 s. Bar, 2  $\mu\text{m}$ .

The method described in this paper could be extended to examining the effects of regulatory proteins and different  $\sigma$ -factors on the interactions of DNA-RNA polymerase and the elementary process of transcription directly at the single molecule level. Furthermore, this method could be applied to the study of other DNA binding proteins, such as helicase and restriction endonuclease.

We thank Dr. O. Ohara for helpful discussions and Dr. A. H. Iwane and colleagues of the ERATO project for advice and encouragement. We thank Dr. J. West, and Dr. K. Kinoshita, Jr., for critically reading the manuscript and for valuable discussions.

## REFERENCES

- Berliner, E., E. C. Young, K. Anderson, H. K. Mahtani, and J. Gelles. 1995. Failure of a single-headed kinesin to track parallel to microtubule protofilaments. *Nature*. 373:718–721.
- Berg, H. 1983. *Random Walks in Biology*. Princeton University Press, Princeton, NJ.
- Cluzel, P., A. Lebrun, C. Heller, R. Lavery, J.-L. Viovy, D. Chatenay, and F. Caron. 1996. DNA: an extensible molecule. *Science*. 271:792–794.
- Craig, M. L., W.-C. Sch, and M. T. Record, Jr. 1995. HO- and DNase I probing of *E. coli* RNA polymerase- $\lambda$   $P_R$  promoter open complexes:  $\text{Mg}^{2+}$  binding and its structural consequences at the transcription. *Biochemistry*. 34:15624–15632.
- Finer, J. T., R. M. Simmons, and J. A. Spudis. 1994. Single myosin molecule mechanics: piconewton forces and nanometre steps. *Nature*. 368:113–119.

- Funatsu, T., Y. Harada, M. Tokunaga, K. Saito, and T. Yanagida. 1995. Imaging of single fluorescent molecules and individual ATP turnovers by single myosin molecules in aqueous solution. *Nature*. 374:555–559.
- Giladi, H., K. Murakami, A. Ishihama, and A. B. Oppenheim. 1996. Identification of an UP element within the IHF binding site at the  $P_L1$ - $P_L2$  tandem promoter of bacteriophage  $\lambda$ . *J. Mol. Biol.* 260:484–491.
- Harada, Y., T. Funatsu, M. Tokunaga, Y. Ishii, and T. Yanagida. 1998. Single molecule imaging and nano-manipulation of biomolecules. *Methods Cell Biol.* 55:117–128.
- Harada, Y., K. Sakurada, T. Aoki, D. D. Thomas, and T. Yanagida. 1990. Mechanochemical coupling in actomyosin energy transduction studied by in vitro movement assay. *J. Mol. Biol.* 216:49–68.
- Higuchi, H., E. Muto, Y. Inoue, and T. Yanagida. 1997. Kinetics of force generation by single kinesin molecules activated by laser photolysis of caged ATP. *Proc. Natl. Acad. Sci. USA*. 94:4395–4400.
- Igarashi, K., and A. Ishihama. 1991. Bipartite functional map of the *E. coli* RNA polymerase  $\alpha$  subunit: involvement of the C-terminal region in transcription activation by cAMP-CRP. *Cell*. 65:1015–1022.
- Ishijima, A., H. Kojima, T. Funatsu, M. Tokunaga, H. Higuchi, H. Tanaka, and T. Yanagida. 1998. Simultaneous observation of individual ATPase and mechanical events by a single myosin molecule during interaction with actin. *Cell*. 92:161–171.
- Iwane, A. H., T. Funatsu, Y. Harada, M. Tokunaga, O. Ohara, S. Morimoto, and T. Yanagida. 1997. Single molecular assay of the individual ATP turnovers by a myosin-GFP fusion protein expressed in vitro. *FEBS Lett.* 407:235–238.
- Kabata, H., O. Kurosawa, I. Arai, M. Washizu, S. A. Margaron, R. E. Glass, and N. Shimamoto. 1993. Visualization of single molecules of RNA polymerase sliding along DNA. *Science*. 262:1561–1563.
- Kasas, S., N. H. Thomson, B. L. Smith, H. G. Hansma, X. Zhu, M. Guthold, C. Bustamante, E. T. Kool, M. Kashlev, and P. K. Hansma. 1997. *Escherichia coli* RNA polymerase activity observed using atomic force microscopy. *Biochemistry*. 36:461–468.
- Matsumoto, S., K. Morikawa, and M. Yanagida. 1981. Light microscopic structure of DNA in solution studied by the 4',6-diamidino-2-phenylindole staining method. *J. Mol. Biol.* 152:501–516.
- McClure, W. R. 1985. Mechanism and control of transcription initiation in prokaryotes. *Annu. Rev. Biochem.* 54:171–204.
- Perkins, T. T., D. E. Smith, and S. Chu. 1994. Direct observation of tube-like motion of a single polymer chain. *Science*. 264:819–822.
- Polyakov, A., E. Severinova, and S. A. Darst. 1995. Three-dimensional structure of *E. coli* core RNA polymerase: promoter binding and elongation conformations of the enzyme. *Cell*. 83:365–373.
- Rees, W. A., R. W. Keller, J. P. Vesenska, G. Yang, and C. Bustamante. 1993. Evidence of DNA bending in transcription complexes imaged by scanning force microscopy. *Science*. 260:1646–1652.
- Ricchetti, M., W. Metzger, and H. Heumann. 1988. One-dimensional diffusion of *Escherichia coli* DNA-dependent RNA polymerase: a mechanism to facilitate promoter location. *Proc. Natl. Acad. Sci. USA*. 85:4610–4614.
- Rippe, K., M. Guthold, P. H. von Hippel, and C. Bustamante. 1997. Transcriptional activation via DNA looping: visualization of intermediates in the activation pathway of *E. coli* RNA polymerase  $\cdot \sigma^{54}$  holoenzyme by scanning force microscopy. *J. Mol. Biol.* 270:125–138.
- Schafer, D. A., J. Gelles, M. P. Sheetz, and R. Landick. 1991. Transcription by single molecules of RNA polymerase observed by light microscopy. *Nature*. 352:444–448.
- Singer, P., and C.-W. Wu. 1987. Promoter search by *Escherichia coli* RNA polymerase on a circular DNA template. *J. Biol. Chem.* 262:14178–14189.
- Smith, S. B., Y. Cui, and C. Bustamante. 1996. Overstretching B-DNA: the elastic response of individual double-stranded and single-stranded DNA molecules. *Science*. 271:795–799.
- Spolar, R. S., and M. T. Record, Jr. 1994. Coupling of local folding to site-specific binding of proteins to DNA. *Science*. 263:777–784.
- Svoboda, K., C. F. Schmidt, B. J. Schnapp, and S. M. Block. 1993. Direct observation of kinesin stepping by optical trapping interferometry. *Nature*. 365:721–727.

- Tang, Y., K. Murakami, A. Ishihama, and P. L. deHaseth. 1996. Upstream interactions at the lambda  $P_{RM}$  promoter are sequence-nonspecific and activate the promoter to a lesser extent than an introduced UP element of an rRNA promoter. *J. Bacteriol.* 178:6945–6951.
- Tokunaga, M., K. Kitamura, K. Saito, A. H. Iwane, and T. Yanagida. 1997. Single molecule imaging of fluorophores and enzymatic reactions achieved by objective-type total internal reflection fluorescence microscopy. *Biochem. Biophys. Res. Commun.* 235:47–53.
- Tsuda, Y., H. Yasutake, A. Ishijima, and T. Yanagida. 1996. Torsional rigidity of single actin filaments and actin-actin bound breaking force under torsion measured directly by in vitro micromanipulation. *Proc. Natl. Acad. Sci. USA.* 93:12937–12942.
- Vale, R. D., T. Funatsu, L. Romberg, D. W. Pierce, Y. Harada, and T. Yanagida. 1996. Direct observation of single kinesin molecules moving along microtubules. *Nature.* 380:451–453.
- von Hippel, P. H., and O. G. Berg. 1989. Facilitated target location in biological systems. *J. Biol. Chem.* 264:675–678.
- Wang, M. D., H. Yin, R. Landrick, J. Gelles, and S. M. Block. 1997. Stretching DNA with optical tweezers. *Biophys. J.* 72:1335–1346.
- Werner, M. H., A. M. Gronenborn, and G. M. Clore. 1996. Interaction, DNA kinking, and the control of transcription. *Science.* 271:778–784.
- Yin, H., M. D. Wang, K. Svoboda, R. Landick, S. M. Block, and J. Gelles. 1995. Transcription against an applied force. *Science.* 270:1653–1657.